INITIATION COD AS A FRACTURE CRITERION FOR ZR-2.5% Nb PRESSURE TUBE ALLOY

L. A. Simpson*

INTRODUCTION

The CANDU† nuclear reactor system uses pressure tubes of 20% cold-worked Zr-2.5% Nb to contain the heavy water coolant. Fracture prediction is based on a critical crack length at operating temperature which has been determined by burst testing full size tube sections under various operating conditions [1]. A reliable means of predicting critical crack lengths from tests on small specimens would greatly reduce the cost and effort in this area. To achieve this, a geometry independent parameter which signals crack propagation must be identified and must be calculable from the applied forces on the geometry of interest. In materials such as Zr-2.5% Nb where crack propagation is accompanied by considerable plasticity, geometry independent fracture criteria are still under development. δ_m, the crack opening displacement (COD) at instability (maximum load) has been studied as a possible fracture criterion for zirconium alloys [2, 3]. However, measurements on small specimens and tubes were not always in agreement [4] which may indicate a geometry dependence for δ_m. More recently, workers using COD methods have been studying δ_i, the COD for crack initiation, which shows much more geometry independence than δ_m, at least for steels [5]. δ_i can often be much smaller than δ_m depending on the amount of stable crack growth a specimen will accommodate. Attainment of δ_i at a flaw in a structure does not necessarily indicate failure and it therefore may be too conservative to be practical as a fracture criterion. However, this decision must await a characterization of δ_i for a given material.

Zirconium has a low solubility for hydrogen which results in the precipitation of zirconium hydride platelets at low temperatures. As-received Zr-2.5% Nb pressure tube material contains ∿10 μg/g [H] which exceeds solubility below about 150°C. At reactor operating temperatures (240 - 290°C), the solubility is 35 to 60 μg/g [6]** and it is possible that this level could be exceeded during a reactor lifetime. Hydride has an embrittling effect on zirconium alloys, especially if the platelets lie in the potential crack plane. However, as a result of the extrusion and cold working during tube fabrication, the platelets are oriented with their normals in the radial direction where their effect on the propagation of through-thickness cracks is weak. A significant effect on fracture resistance still exists at room temperature although, at operating temperatures, it becomes negigble for hydrogen concentrations up to at least 400 μg/g [1, 4, 7]. This work characterizes the crack initiation process in Zr-2.5%

* Atomic Energy of Canada Limited, Pinawa, Manitoba, Canada.

** Based on an extrapolation of data in reference [6] and unpublished work at WNRE.

† CANDU - CANada Deuterium Uranium - denotes the Canadian design of pressurized heavy water cooled reactor.

Nb pressure tube material at two temperatures and hydrogen levels to assess the suitability of δ_i as a fracture criterion.

EXPERIMENTAL

Compact tension specimens (CTS) were machined from flattened pressure tubing with the crack parallel to the tube axis. Fatigue cracks were induced at the notch root using a maximum stress intensity of 18 MPa.$m^{1/2}$. Referring to the standard nomenclature [8] the dimensions were W = 17.0 mm, a/W = 0.4 and 0.6 and b = 3.75 mm. The latter measurement being just under the pressure tube wall thickness of 4.0 mm. As-received specimens had a hydrogen content of ∿10 μg/g [H]. Some of these specimens were gaseously hydrided at 400°C to a concentration of 200 μg/g followed by a homogenization treatment at 400°C for one week in a sealed, evacuated capsule. The temperature 400°C was chosen to prevent microstructural changes.

COD at 20°C was determined using a clip gauge at the crack mouth combined with a calibration for the CTS specimen geometry relating clip gauge displacement to COD. The calibration technique was similar to that used by Ingham et al [9]. Plots of crack face displacement (determined photographically during loading) against distance to the crack tip were extrapolated to the crack tip location to give COD for a series of load levels. Separate calibrations were made for a/W = 0.4 and 0.6. To determine δ_i, identical specimens were loaded to various COD values between an estimated δ_i and δ_m. They were then heat-tinted at 300°C to identify the stable crack growth and broken open. Extrapolation of plots of COD against the maximum extent of stable crack growth, Δa, to Δa = 0 yielded δ_i [10].

The fracture surfaces were examined in a scanning electron microscope and the sizes of stretch zones, the distances between the fatigue cracks and the stable crack features, were measured. It has been demonstrated for a number of materials that stretch zone size is closely related to COD [11]. The heights of the stretch zones normal to the fracture surface were measured, doubled to account for both halves of the specimen, and compared to δ_i as determined above. This technique was the only one used on specimens tested at 240°C to estimate δ_i since the testing furnace would not accommodate a clip gauge. These specimens were simply pulled to just under maximum load, heat tinted and broken open at room temperature.

RESULTS

Tests at 20°C

Measurements of δ_m on specimens of a/W = 0.4 and 0.6 yielded values of 0.25 and 0.18 mm respectively for as received material at room temperatures which indicates a geometry dependence for this parameter.

Figure 1 shows the COD plotted against stable crack length for both as received and hydrided material at 20°C (a/W = 0.6). The effect of hydrogen on δ_i is clear with δ_i reduced from about 0.050 mm to 0.022 mm by 200 μg/g of hydrogen. In Figures 2a and b, the fracture surfaces near the point of crack initiation are shown. At 20°C in as-received material the stretch zones were fairly uniform in size within the specimen thickness but increased somewhat near the surface. Since crack initiation took place near the specimen midsection, all measurements were made in the specimen

interior. There are some areas in Figure 2a where the stretch zone is broken or falls away to a much smaller size. Examination of the other half of the specimen revealed corresponding interruptions in the stretch zone which eliminated the possibility that these features resulted from a deviation of the crack front in the direction normal to the crack plane. Hence, these regions represented local failures early in the development of the stretch zone and they were not included in the stretch zone size measurements.

The interruptions in the stretch zone for hydrided material are much more numerous, Figure 2b, but the same measurement procedure was used.

The height of the stretch zone normal to the crack plane was calculated from measurements on photographs and doubled to give an estimate of δ_i (in initial work, measurements on both halves of a specimen yielded identical results). A summary is given in Table 1 which shows that the two methods of determining δ_i are in good agreement.

The effect of hydrogen on fracture mode is very marked at 20°C. The stable crack growth surface in Figure 2a consists of ductile ridging running in the direction of crack propagation separated by rounded grooves or valleys. Some of these valleys intersect the stretch zone at the interruptions described above. The stable crack growth in the hydrided material, Figure 2b, consists of much narrower ridges separated by fissures running deeply into the crack face. These fissures frequently correspond to interruptions in the stretch zone.

Additional measurements on as-received material at 20°C with a/W = 0.4 also yielded δ_i ∿0.050 mm suggesting that δ_i is more geometry independent than δ_m.

Tests at 240°C

Estimates of δ_i from stretch zones are included in Table 1. Allowing for the overlapping of the standard deviations, there is little significant difference in δ_i between as-received and hydrided material. In fact, δ_i at 240°C, is very similar to that for as-received material at room temperature. Fracture surfaces for stable crack growth are also similar for these three conditions (Figures 2a, c and d).

DISCUSSION

The microstructure of Zr-2.5% Nb normal to the tube axial direction is shown in Figure 3a. It consists of elongated grains of α-zirconium in a continuous grain boundary network of β-zirconium. The grains are also elongated in the direction of crack propagation (axial) as can be seen from the texture of the fatigue crack surfaces in Figure 2. From the dimensions of these features it follows that, while the stable fracture features in Figure 2 reflect the general microstructural morphology, their scale is about an order of magnitude larger. The initiation of fracture in as-received material at 20°C and in both materials at 240°C, appears to have commenced with the nucleation of voids ahead of the stretch zone which grew rapidly in the propagation direction forming the valley. This is reflected in Figure 3b showing a row of voids ahead of a propagating crack. Occasionally a void, nucleating very close to the crack tip, may have broken through to the surface, thus causing an interruption of a stretch zone. The ligaments between the valleys either necked down and

failed by shear if they were thin enough or, alternatively, by void nucleation and coalescence. It is tempting to identify hydride platelets as the source of void nucleation. However, no hydride would have been present at 240°C in the as-received material and its stable fracture features are similar to those for the specimens in Figures 2a and d where it was present. Hence the void nucleation points were probably areas of weakness in the microstructure. Cold worked Zr-2.5% Nb has little work hardening potential and it is conceivable that it could be exhausted in some local regions where under the triaxial stress conditions near the crack tip, void nucleation would readily occur.

Hydride at 20°C has a marked effect on fracture mode. The deep fissures are consistent with the spacing and size of the large hydride platelets oriented normal to the crack plane (Figure 3c). These platelets appear to have fractured under the transverse crack tip stresses early in the specimen loading history i.e. before the development of the stretch zone. The ridges between the fissures appear more jagged in Figure 2b but examination at higher magnification revealed ductile features. While hydride was also present at 20°C in as-received material the platelets were smaller and sparse and did not exert a strong influence on the fracture mode.

At 240°C the hydrided specimens should have contained considerable hydride but it did not appear to have a strong influence on the fracture mode or δ_i. This is consistent with pressure tube burst test results [1] where hydride has little effect on critical crack length at reactor operating temperatures. This behaviour has been attributed to the hydride becoming ductile above 150°C. While there is some indirect evidence in support of this concept [12], recent fracture toughness measurements on pure hydride [13] suggest that it remains brittle at least up to 400°C. Hence the explanation may simply involve the increased ductility of the zirconium and a possible reduction in hydride-matrix interfacial strains at 240°C allowing greater strain accommodation at the crack tip.

CONCLUSIONS

1) δ_i can easily be determined by stretch zone measurement in Zr-2.5% Nb and is influenced by temperature and hydrogen in the same fashion as burst testing data.
2) Fracture initiation in this material is by void nucleation and coalescence and the fracture features reflect the highly textured microstructure.
3) Hydride does not appear to be a major factor in fracture initiation except when it exists in large quantities at 20°C.
4) δ_i appears to be more geometry independent than δ_m and further development of this parameter as a fracture criterion is justified.

REFERENCES

1. LANGFORD, W. J. and MOODER, L. E. J., J. Nuclear Materials 39, 1971.
2. FEARNEHOUGH, G. D. and WATKINS, B., Int. J. Fract. Mech. 4, 1968, 233.
3. HENRY, B., Euratom Report EUR 5017f, Ispra, 1973.
4. PICKLES, B. W., Canadian Metallurgical Quarterly, 11, 1972, 139.
5. FEARNEHOUGH, G. D., LEES, G. M. LOWES, J. M. and WEINER, R. T., Practical Application of Fracture Mechanics to Pressure Vessel Technology, Inst. Mech. Eng. London, 1971, 119.

6. KEARNS, J. J., J. Nuclear Materials, 27, 1968, 64.
7. WATKINS, B., COWAN, A., PARRY, G. W. and PICKLES, B. W., ASTM STP 458, 1969, 141.
8. Annual Book of ASTM Standards, Amer. Soc. Test. Mater., Philadelphia, E399-72.
9. INGHAM, T., EGAN, G. R., ELLIOTT, D. and HARRISON, T. C., Practical Applications of Fracture Mechanics to Pressure Vessel Technology, Inst. Mech. Eng. London, 1971, 200.
10. SMITH, R. F. and KNOTT, J. F., Practical Applications of Fracture Mechanics to Pressure Vessel Technology, Inst. Mech. Eng. London, 1971, 65.
11. HARRIS, D. and ELLIOTT, D., Conf. on the Mechanics and Physics of Fracture, Cambridge, U.K., 6-8 Jan., 1975.
12. PARRY, G. W. and EVANS, W., Nucleonics, 22, 1964, 65.
13. SIMPSON, L. A., unpublished work.

Table 1 Results of δ_i Measurements on Compact Tension Specimens a/W=0.6

Temp °C	Hydrogen µg/g	δ_i (Figure 1) (mm.)	δ_i (stretch zone) (mm.)
20	10	0.050	0.054 ± 005
20	200	0.022	0.026 ± 003
240	10	-	0.046 ± 006
240	200	-	0.056 ± 008

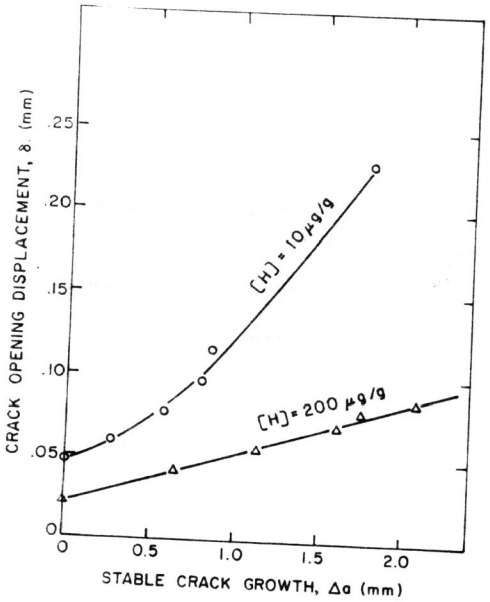

Figure 1 Effect of Stable Crack Growth on COD

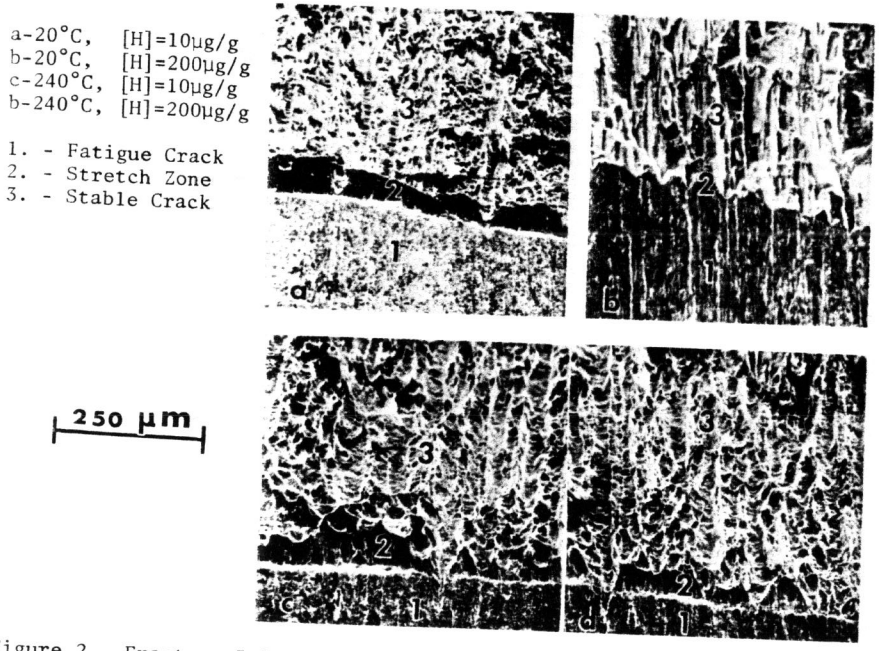

Figure 2 Fracture Initiation Regions for Various Test Conditions

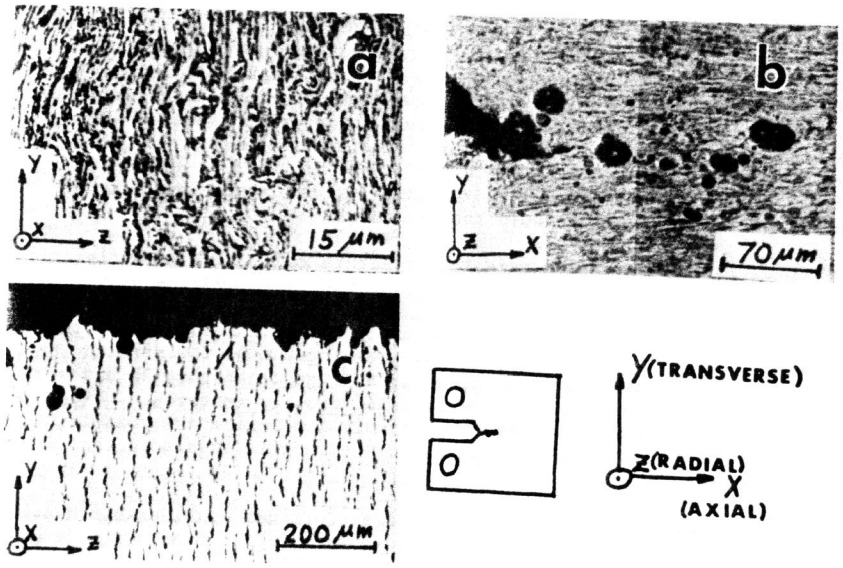

Figure 3 Microstructural details of Zr-2.5% Nb: (a) grain structure, (b) crack tip void development, (c) hydride orientation (200 μg/g).